J. Biochem. **134**, 599–606 (2003)
DOI: 10.1093/jb/mvg178

Mutagenesis of the Dimer Interface Region of *Corynebacterium callunae* Starch Phosphorylase Perturbs the Phosphate-Dependent Conformational Relay that Enhances Oligomeric Stability of the Enzyme

Bernd Nidetzky*[,1], Richard Griessler[1], Francesco-Maria Pierfederici[1,3], Barbara Psik[1], Andrea Sciré[2] and Fabio Tanfani[2]

[1]Institute of Biotechnology, Graz University of Technology, Petersgasse 12/I, A-8010 Graz, Austria; and [2]Institute of Biochemistry, Faculty of Sciences, Università Polytecnica delle Marche, Via Ranieri 60131 Ancona, Italy; and [3]Department of Chemical Sciences, University of Catania, 95125 Catania, Italy

Received June 16, 2003; accepted August 6, 2003

We have used alanine-scanning site-directed mutagenesis of the dimer contact region of starch phosphorylase from *Corynebacterium callunae* to explore the relationship between a protein conformational change induced by phosphate binding and the up to 500-fold kinetic stabilization of the functional quarternary structure of this enzyme when phosphate is present. Purified mutants (at positions Ser-224, Arg-226, Arg-234, and Arg-242) were characterized by Fourier transform-infrared (FT-IR) spectroscopy and enzyme activity measurements at room temperature and under conditions of thermal denaturation. Difference FT-IR spectra of wild type and mutants in ^2H_2O solvent revealed small changes in residual amide II band intensities at ≈ 1,550 cm^{-1}, indicating that $^1H/^2H$ exchange in the wild type is clearly perturbed by the mutations. Decreased $^1H/^2H$ exchange in comparison to wild type suggests formation of a more compact protein structure in S224A, R234A, and R242A mutants and correlates with rates of irreversible thermal denaturation at 45°C that are up to 10-fold smaller for the three mutants than the wild type. By contrast, the mutant R226A inactivates 2.5-fold faster at 45°C and shows a higher $^1H/^2H$ exchange than the wild type. Phosphate (20 mM) causes a greater change in FT-IR spectra of the wild type than in those of S224A and 234A mutants and leads to a 5-fold higher stabilization of the wild type than the two mutants. Therefore, structural effects of phosphate binding leading to kinetic stability of wild-type starch phosphorylase are partially complemented in the S224A and R234A mutants. Infrared spectroscopic measurements were used to compare thermal denaturations of the mutants and the wild type in the absence and presence of stabilizing oxyanion. The broad denaturation transition of unliganded wild type in the range 40–50°C is reduced in the S224A and R234A mutants, and this reflects mainly a shift of the onset of denaturation to a 4–5°C higher value.

Key words: dimer interface, FT-IR spectroscopy, long-range interactions, oligomeric structure, starch phosphorylase.

Abbreviations: Amide I′, amide I band in ^2H_2O medium; FT-IR, Fourier transform-infrared; GP, glycogen phosphorylase; OTD, onset of thermal denaturation; P_i, inorganic phosphate; StP, wild-type starch phosphorylase from *Corynebacterium callunae*; recStP, recombinant wild-type StP expressed in *E. coli*; his_6-recStP, recStP harboring an N-terminal metal-affinity fusion peptide containing six histidines; T_m, melting temperature.

It is common for an enzyme to be stabilized by extrinsic ligands. However, the mechanism by which ligand binding induces a stabilized protein conformation is often very complex. Manipulating stability through "conformation engineering" is thus a challenging approach to make an enzyme more suitable for biotechnological applications (*e.g.*, *1*, *2*). Among reports of enzyme stabilization by moderate-affinity ligands, the stability-enhancing effect of phosphate in starch phosphorylase (StP) from *Corynebacterium callunae* is outstanding because of its magnitude (*3*, *4*). Therefore, examining the conformational effect through which binding energy from the interactions with phosphate is translated into an up to 500-fold kinetically more stable structure seems to be particularly significant for this enzyme.

StP belongs to the glycogen phosphorylase (GP) family of enzymes (*5*, *6*) and is a dimer composed of two identical subunits of ≈88,000 molecular weight (*5*, *7*). In dilute solution, the functional quartenary structure of StP is rapidly lost by dissociation of the protomers. Physiological levels of phosphate (≥5 mM) inhibit the dissociative step and hence delay the loss of enzyme activity (*3*, *4*). Phosphate binding to a saturable oxyanion site, which is different from the part of the active site that recognizes the phosphate group in phosphorylase substrates, induces a conformational change in protein structure,

*To whom correspondence should be addressed. Tel: +43-316-873-8400, Fax: +43-316-873-8434, E-mail: bernd.nidetzky@tugraz.at

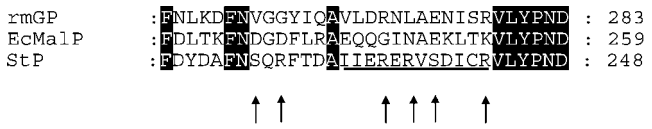

Fig. 1. **Comparison of the TOWER α-helix region in primary structures of maltodextrin phosphorylase from *E. coli* (EcMalP) (*8*), glycogen phosphorylase from rabbit muscle (rmGP) (*9*, *10*), and StP.** The position of the TOWER helix, which is part of the dimer interface, is underlined in bold. Side-chains of StP replaced by a methyl side-chain of alanine are indicated by arrows. Amino acids for site-directed mutagenesis were selected on the basis of side-chain propensity to occur in phosphate sites in proteins (*11*). In rmGP, the region (residues 252–266) going into the TOWER helix is not well ordered. In EcMalP, the same region (residues 228–241) forms a short helix (residues 228–236) and an irregular helix (residues 237–241) which both have substantial intersubunit contacts (see Refs. *8* and *9*). In StP, a structural assignment is not possible for the region leading into the TOWER helix.

which seems to be crucial to tightened intersubunit contacts. Changes in cofactor environment at the active site, decreases in the extent of $^1H/^2H$ exchange at equilibrium in ^2H_2O buffer, and small increases in the relative content of α-helical secondary structure serve as reporters of formation of a globally more compact protein structure when phosphate is present. The observed structural rearrangements likely involve changes in dimer contacts and intrasubunit interactions (*3*).

The present paper aims at exploring causal relationships between structural changes in the interfacial region of StP, dimer stability, and stabilization thereof by phosphate. The work expands upon the recent finding (*5*) that stability of StP is dependent on the conformations of Arg-234 and Arg-242. Secondary structure assignment on the basis of multiple sequence alignment of StP and other GPs revealed that Arg-234 and Arg-242 are both contributed by an α-helix that forms a common and positionally conserved element of the known dimer interfaces of GPs (*5*; Fig. 1). We therefore turned our attention specially to the region of the subunit-to-subunit interface of StP and report here production of three new enzyme variants by using alanine-scanning site-directed mutagenesis. The mutated amino acids were selected because their side chains occur frequently at protein sites which interact with phosphate or phosphorylated ligands (*11*). We utilized Fourier transform-infrared (FT-IR) spectroscopy at room temperature to characterize structural properties of four mutants (Ser-224, Arg-226, Arg-234, Arg-242; see Fig. 1) that show phosphate-dependent stabilities clearly different from that of the wild type. Changes in protein conformation caused by the mutations were identified and correlated with differences in thermal denaturation rates of wild type and the mutants in the absence and presence of phosphate, as monitored by FT-IR spectroscopy and enzyme activity. The results are novel and significant in several respects. First of all, they identify amino acid side chains in StP whose replacement by the methyl side chain of alanine partially complements the effect of phosphate in the wild type. Second, they allow us to distinguish a conformational change induced by phosphate binding that stabilizes the native dimer structure of StP, from another that delays melting of the protein structural core at high temperatures. Third, they reveal that certain mutations increase, in comparison to wild type, the connectivity between loss of oligomeric integrity and unfolding under conditions of thermal denaturation.

EXPERIMENTAL PROCEDURES

Materials—Materials for protein chromatography and all components of enzyme assays were reported elsewhere (*3*, *4*, *7*). Deuterium oxide (99.9% ^2H_2O), ^2HCl and NaO^2H were purchased from Aldrich. All the other chemicals were commercial samples of the purest quality.

Mutagenesis—Site-directed replacements by alanine of Arg-234, Arg-236, and Arg-242 have been described recently (*5*). Single point mutations into alanine at positions Ser-224, Arg-226, and Ser-238 were introduced by the PCR-based overlap extension method using as the template a 1,400-bp fragment of the stP gene, obtained by digestion of the plasmid vector pQE 30-stP (*5*) with Sph I and Eco 91I. The following mutagenic oligonucleotide primers (and their corresponding reverse complementary primers) were used where the mismatched bases are underlined:

5′-GCCTTCAACGCACAGCGC-3′ (S224A);
5′-TCACAGGCCTTTACGGAC-3′ (R226A);
5′-CGCGTTGCCGATATCTGC-3′ (S238A).

PCR was carried out under conditions reported previously (*5*). Plasmid mini-prep DNA was subjected to dideoxy sequencing to verify that the desired mutation had been introduced and that no misincorporation of nucleotides had occurred as a result of the DNA polymerase. Each mutagenized fragment was then cloned into the residual pQE 30-stP vector.

Enzyme Preparation and Characterization—Wild-type and mutated stP genes were expressed in *E. coli* XL1 Blue using reported procedures (*5*). All recombinant enzymes, wild-type or mutant, carried an N-terminal dodecapeptide fusion (RGSHHHHHHGSA) that served as a metal affinity tag for purification. The abbreviation his_6-recStP is chosen to indicate this fact for the recombinant wild-type enzyme. The comparative examination of his_6-recStP and mutants thereof is based on the experimental observation (*5*) that the N-terminal fusion does not *per se* alter functional properties related to activity, stability, and stabilization of the enzyme. All enzymes were isolated using a protocol described recently (*5*). Isolated proteins migrated as single bands to identical positions in SDS PAGE. Semi-quantitative densitometric analysis of Coomassie Blue–stained gels showed that each protein was at least 95% pure. Protein was determined using the Bio-Rad dye binding method with wild-type StP as standard.

Recombinant enzymes were assayed for specific activity in direction of starch phosphorolysis and for cofactor content, using reported protocols (*5*, *7*). For each protein, the elution profile in a Superose 12 column sizing experiment was determined (*5*). Inactivation rates of his_6-recStP and mutants were compared at 45°C in the absence and presence of the indicated concentration of potassium phosphate or potassium sulfate using standardized conditions that have been detailed elsewhere (*3*, *5*).

Infrared Measurements and Infrared Spectra—Typically, 1.5 mg of protein, was analyzed in three different buffers prepared in ^2H_2O, p^{2}H 6.8. The buffers used were

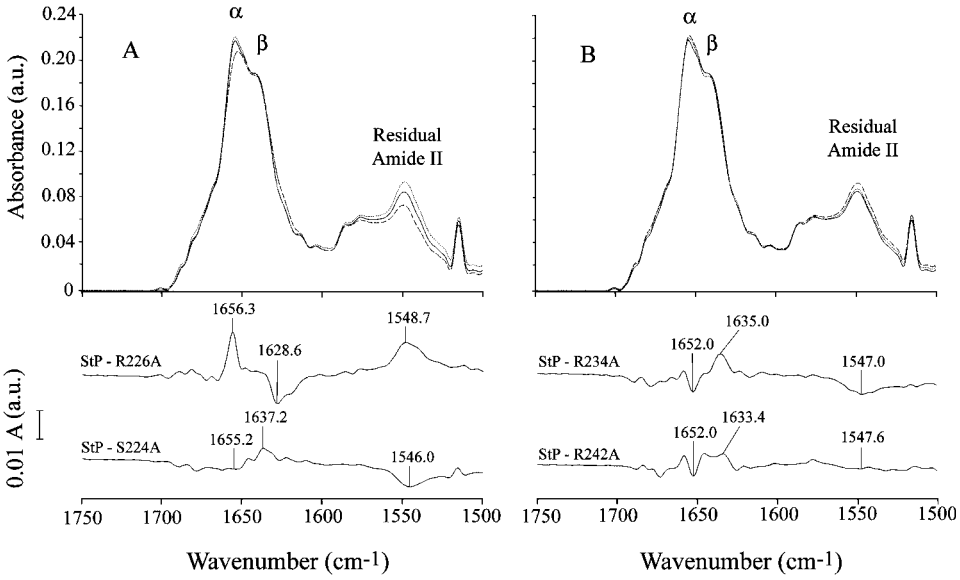

Fig. 2. **Comparison of spectra of his$_6$-recStP and mutants thereof in 2 mM P$_i$ buffer.** Spectra were obtained at 20°C in ^2H_2O medium, p^{2}H 6.8. Top of panel (A): continuous, dashed and dotted lines represent the deconvoluted spectra of his$_6$-recStP, R226A and S224A, respectively. Top of panel (B): continuous, dashed and dotted lines represent the deconvoluted spectra of his$_6$-recStP, R234A and R242A, repectively. Bottom of panels (A) and (B): difference spectra obtained by subtracting the respective mutant spectrum from the spectrum of his$_6$-recStP, as indicated in the figure.

sodium phosphate at 2 mM (buffer A) or 20 mM concentration (buffer B), or 20 mM Hepes plus 20 mM sodium sulfate (buffer C). Buffer exchange and concentration of protein solutions were performed as described elsewhere (*3*). A final volume of approximately 40 μl was used for FT-IR spectroscopic analysis at 20°C and during a thermal denaturation experiment, as reported in detail for StP (*3*). All spectra were collected and processed using SPECTRUM software from Perkin Elmer. Correct substraction of H_2O was judged to yield an approximately flat baseline at 1,900–1,400 cm^{-1}, and subtraction of ^2H_2O was adjusted to the removal of the bending absorption close to 1,220 cm^{-1} (*12*, *13*). The absorbance spectra were normalized to the same amide I′ band (1,700–1,600 cm^{-1}) area and then processed to obtain resolution-enhanced and difference spectra. The deconvoluted parameters were set with a gamma value of 2.5 and a smoothing length of 60. Second derivative spectra were calculated over a 9-data-point range (9 cm^{-1}).

RESULTS AND DISCUSSION

Preparation and Characterization of S224A, R226A, and S238A Mutants—The S224A, R226A, and S238A mutants were expressed in *E. coli* and purified to apparent electrophoretic homogeneity (not shown) in a yield of 32%, 28%, and 35%, respectively. All proteins contained approximately 0.9 moles of pyridoxal 5′-phosphate per mole of 88-kDa protein subunit. The specific enzyme activities of S224A, R226A, and S238A mutants (≈ 26 U/mg), measured in the direction of phosphorolysis, were closely similar to the specific activity of his$_6$-recStP. In a column sizing experiment, the elution profiles of his$_6$-recStP, S224A, R226A, and S238A were almost superimposable. During an initial screening, the inactivation rates of the purified mutants were assessed in comparison to his$_6$-recStP using an irreversible thermal denaturation experiment at 45°C (*5*). S224A and R226A together with the previously reported R234A and R242A (*5*) were selected for structural characterization by FT-IR spectroscopy because their kinetic stabilities in the absence or presence of 50 mM of phosphate were significantly different from that of his$_6$-recStP (see later). By contrast, S238A and his$_6$-recStP are not different under these conditions of inactivation.

Conformational Changes in Protein Structure Induced by Mutation—The absorbance, deconvoluted and second derivative spectra of his$_6$-recStP in 20 mM sodium phosphate buffer (data not shown) are very similar to the previously reported spectra of StP recorded in 50 and 100 mM phosphate buffer (*3*). In particular, comparison of spectra of his$_6$-recStP and StP reveals that the α-helix band (1,655.5 cm^{-1}) and the β-sheet band (1,640.8 cm^{-1}) display similar positions and a similar band intensity ratio (see Ref. *3* for detailed band assignments), indicating close similarity in secondary structural composition of StP and his$_6$-recStP. In this previous paper (*3*), we also showed that the FT-IR spectra of StP recorded in ^2H_2O solvent in the absence and in the presence of 2 mM P$_i$ are the same, indicating that this low P$_i$ concentration does not detectably affect the secondary structure and the ^{1}H/^{2}H exchange ability of the protein. Hence, this implies that in 2 mM P$_i$ buffer, observable differences in mutant spectra with respect to the spectrum of the wild type are due to the mutations only. The deconvoluted spectra of the S224A and R226A mutants and the R234A and R242A mutants, in 2 mM P$_i$ buffer, are shown in Fig. 2, A and B, respectively. In each, the deconvoluted spectrum of his$_6$-recStP is displayed for ease of comparison.

The spectrum of R226A mutant displays a lower intensity of the α-helix band and of the residual amide II band as compared to the control. Also, the position of the α-helix band is lower than that present in the spectrum of his$_6$-recStP. These data indicate that the R226A mutation lowers the content of α-helices and increases the ability of the protein to exchange the amide hydrogens with deuterium. Other small changes in the secondary structure (1,700–1,600 cm^{-1}) induced by the mutation are shown by the difference spectrum, obtained by subtracting the mutant spectrum from the spectrum of his$_6$-recStP (Fig. 2A, bottom panel). Difference spectra allow detection of even tiny differences between two absorbance or resolu-

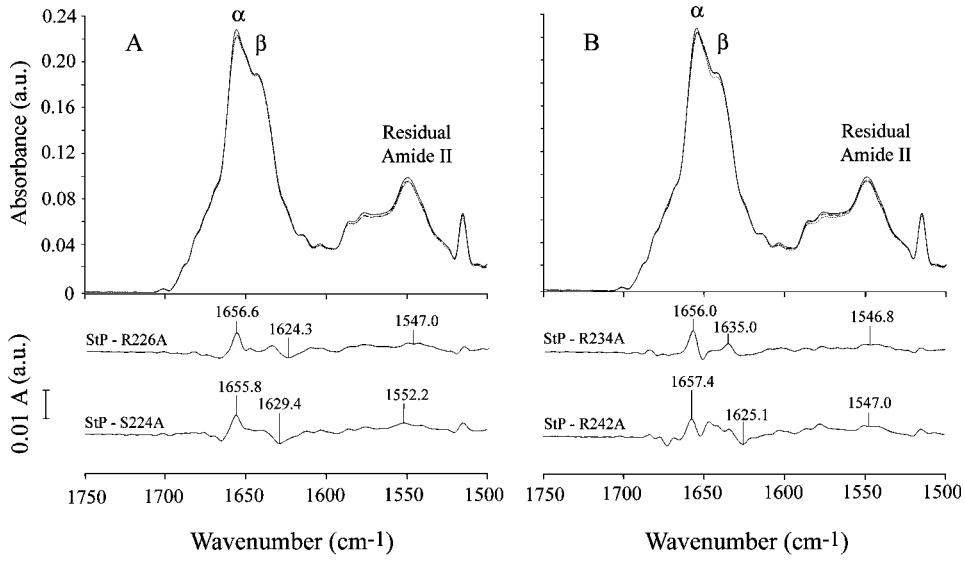

Fig. 3. **Comparison of spectra of his_6-recStP and mutants thereof in 20 mM P_i buffer.** Spectra were obtained at 20°C in ^2H_2O medium, p^{2}H 6.8. Top of panel (A): continuous, dashed and dotted lines represent the deconvoluted spectra of his_6-recStP, R226A and S224A, respectively. Top of panel (B): continuous, dashed and dotted lines represent the deconvoluted spectra of his_6-recStP, R234A and R242A, repectively. In panels (A) and (B), the deconvoluted spectra of R226A and S224A and of R242A and R234A are almost superimposable, respectively. Bottom of panels (A) and (B): difference spectra obtained by subtracting the respective mutant spectrum from the spectrum of his_6-recStP, as indicated in the figure.

tion-enhanced spectra (*14*). It must be emphasized that the small peaks are real and not due to noise or water vapor absorption, because no bands are present in the 1,750–1,700 cm^{-1} region, which is informative for the presence of such absorptions. Positive and negative peaks indicate a higher and lower intensity of a particular band in the spectrum of his_6-recStP than in the mutant spectrum, respectively. The difference spectrum in Fig. 2A indicates a higher intensity of the 1,628.6 cm^{-1} band (β-sheet) and a lower intensity of the 1,548.7 cm^{-1} band (residual amide II band) in the spectrum of the R226A mutant in comparison to the spectrum of his_6-recStP.

Even smaller differences between spectra of his_6-recStP and the remaining mutants are brought to light by deconvoluted and, in particular, difference spectra (Fig. 2, A and B; top and bottom panels). The mutation R242A seems not to affect the secondary structure and the $^1H/^2H$ exchange as the R226A mutation does, since the deconvoluted spectra of his_6-recStP and the R242A mutant are almost the same. The spectra of S224A and R234A mutants show a higher intensity of the residual amide II band and a slightly higher intensity of the α-helix band than the control, indicating that these mutations induce a small increase in the content of α-helices and a lower $^1H/^2H$ exchange in comparison to his_6-recStP. In the case of S224A and R234A mutants, the effect of the mutation is similar to that exerted by a high P_i concentration on StP (*3*). Indeed, it was shown that in StP, the increase of the α-helix band intensity and the extent of $^1H/^2H$ exchange are P_i concentration dependent: the higher the P_i concentration, the higher the α-helix band intensity and the lower the $^1H/^2H$ exchange (or the higher the amide II band intensity) (*3*). As the spectra of S224A and R234A mutants show clearly that there is a lower $^1H/^2H$ exchange in comparison to the control (his_6-recStP), we conclude that these mutations induce a more compact protein structure of the phosphorylase. Judging by $^1H/^2H$ exchange data, replacement of Arg-226 by alanine appears to have the opposite effect on the enzyme.

Results of structural comparison by FT-IR spectroscopy of his_6-recStP and the mutants were corroborated qualitatively by using far-UV CD spectra of the same protein samples (data not shown). However, small differences among his_6-recStP and individual variants detectable by analyzing infrared spectra could not be equally well worked out by comparing the corresponding CD spectra, mainly because of greater reproducibility achieved in infrared experiments. Global parameters of protein structure such as UV absorbance and intrinsic tryptophan fluoresence were very similar for his_6-recStP and mutants thereof. Likewise, fluorescence properties of PLP which are known to be sensitive to polarity of the microenvironment are virtually identical in his_6-recStP and the mutants (not shown). FT-IR spectroscopy was thus used for further characterizations.

Conformational Changes in Structures of his_6-recStP and Mutants Thereof Induced by Oxyanions—FT-IR spectra of his_6-recStP and mutants were recorded in the presence of 20 mM P_i and compared to the corresponding reference spectra, obtained under conditions in which the P_i level was not significant in terms of a structural effect on his_6-recStP. This procedure allowed us to cross-correlate conformational changes that are mainly due to mutation, and others that are caused by a relatively high oxyanion concentration. Spectra of proteins dissolved in 20 mM P_i buffer were identical within the experimental error regarding band positions and band intensities, indicating very similar conformations of his_6-recStP and mutants thereof under these conditions (Fig. 3). Considering the differences between spectra of his_6-recStP and mutants seen clearly under low P_i conditions, this result indicates that the effect of mutation on spectral properties of his_6-recStP is dependent on the P_i concentration and decreases with an increasing level of P_i. An interesting result is borne out upon comparison of spectra of individual mutants obtained in 2 mM and 20 mM P_i buffers (Fig. 4). In S224A and R234A mutants, the two spectra were superimposable, indicating no significant effect of the P_i concentration on conformational properties of the two mutants. Conversely, the α-helix band intensity and $^1H/^2H$ exchange in the R242A and R226A mutants showed a dependence on P_i concentration which was very similar to

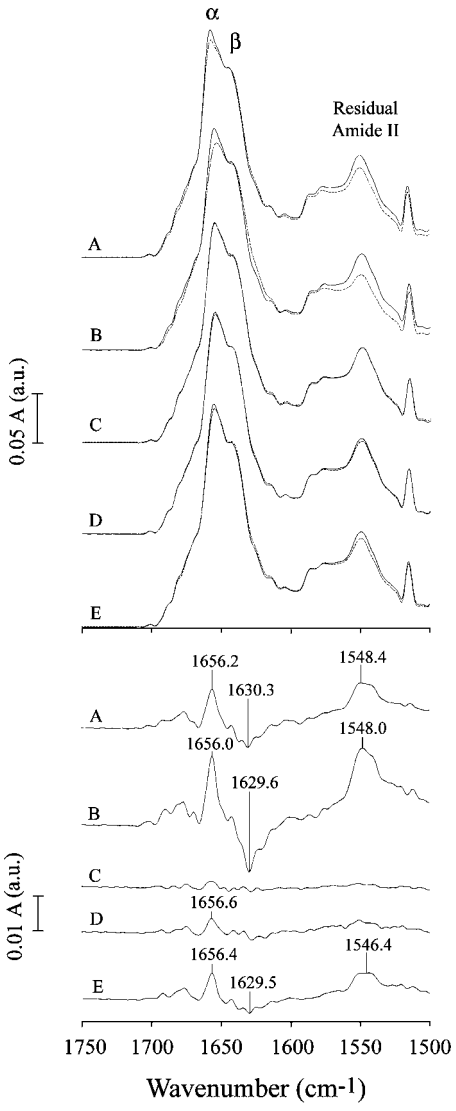

Fig. 4. **Comparison of spectra of his$_6$-recStP and mutants thereof in 2 and 20 mM P$_i$ buffer.** Spectra were obtained at 20°C in ^2H_2O medium, p^{2}H 6.8. Upper set of spectra: comparison of deconvoluted spectra. Continuous and dashed lines represent the spectra obtained in 20 mM P$_i$ and 2 mM P$_i$, respectively. A–E represent spectra of his$_6$-recStP, and of R226A, S224A, R234A and R242A mutants, respectively. Lower set of spectra: difference spectra obtained by subtracting the spectrum obtained in 2 mM P$_i$ from that obtained in 20 mM P$_i$. A and E represent the difference spectra related to his$_6$-recStP, R226A, S224A, R234A, and R242A, respectively.

that of his$_6$-recStP. It is worth noting that protein spectra obtained in 20 mM P$_i$ buffer and in 20 mM Hepes buffer containing 20 mM sulfate were almost indistinguishable from each other in different pairwise comparisons (not shown), suggesting a near-identical effect of the chosen oxyanion levels on the conformation of his$_6$-recStP, irrespective of the amino acid side chain replaced in the mutants. (Note that the dissociation constant (K_d) of the wild-type enzyme-phosphate complex is ≈16 mM and thus 4-fold higher than the corresponding K_d value of the enzyme-sulfate complex (*3*). This suggests a conformational effect of bound phosphate that is greater than that of bound sulfate, in agreement with results of cofactor fluorescence quenching studies (*3*). Therefore, the data imply that Ser-224 and Arg-234 can serve as reporter groups for the structural rearrangements that are induced by oxyanion ligands in his$_6$-recStP. By contrast, Arg-226 is of limited use because its side chain appears to be positioned for a compact StP structure, even when no phosphate is present (Figs. 2A and 3A). However, the fact that the side chain of Arg-242 is destabilizing in the unligated wild type (*5*), whereas its replacement by a methyl group in R242A is spectrally silent within the experimental error under all conditions tested (Fig. 3), clearly indicates that there cannot be a quantitative correlation between the structural compactness inferred from infrared data and the kinetic stability measured at an elevated temperature (see later). Likewise, sulfate is more stabilizing than phosphate in all enzyme assays, but this observation, to be reported later, does not mirror any counterpart changes in infrared spectra of proteins, *i.e.*, in $^1H/^2H$ exchange and secondary structure composition, recorded under different oxyanion conditions. However, thermal stability of proteins in the presence of sulfate, as monitored by infrared spectroscopy, is perfectly consistent with kinetic stability in regard to half life at high temperature.

Analysis by FT-IR Spectroscopy of Thermal Denaturation of his$_6$-recStP and Mutants Thereof—We have monitored changes in the infrared spectra of his$_6$-recStP or mutants thereof during controlled irreversible thermal denaturation experiments in which the temperature was raised in 5°C steps from 20°C to 90°C. Temperature-shift infrared measurements were carried out with proteins dissolved in 2 mM and 20 mM phosphate buffer, and in 20 mM Hepes buffer containing 20 mM sulfate. As shown recently for StP (*3*), the absence of complete cooperativity in the thermal unfolding process requires that spectra recorded over the entire temperature range be scrutinized for structural rearrangements possibly related to loss of the functional oligomeric structure, unfolding, and aggregation induced at a certain temperature. This was done by comparing the deconvoluted spectra recorded at each temperature or using difference spectra calculated from two absorbance spectra recorded in a temperature interval of 5°C. Furthermore, denaturation was also followed by monitoring the amide I′ bandwidth, calculated at 3/4 of the amide I′ band height, as a function of temperature. By combining the three methods of analysis, reasonably precise values (±0.5°C) were obtained for two characteristic temperatures that provide an adequate representation of the denaturation of each protein component under different conditions: the onset of denaturation (OTD) and the melting temperature of the protein (T_m). In the unligated wild type, the observed OTD of ≈35°C appears to reflect the process of subunit dissociation, which has been shown by column-sizing experiments to occur at a significant rate even at 30°C (*3*). The optimum temperature (T_{opt}) for the reverse catalytic reaction of the wild-type enzyme is 35°C under conditions when no stabilizing oxyanion is present. This value of T_{opt} is governed by irreversible inactivation of the enzyme which in the absence of detectable unfolding most likely mirrors the loss of oligomeric structure (*3*). We stress, however, that a correlation between OTD and subunit dissociation is a qualitative one and has to be used with

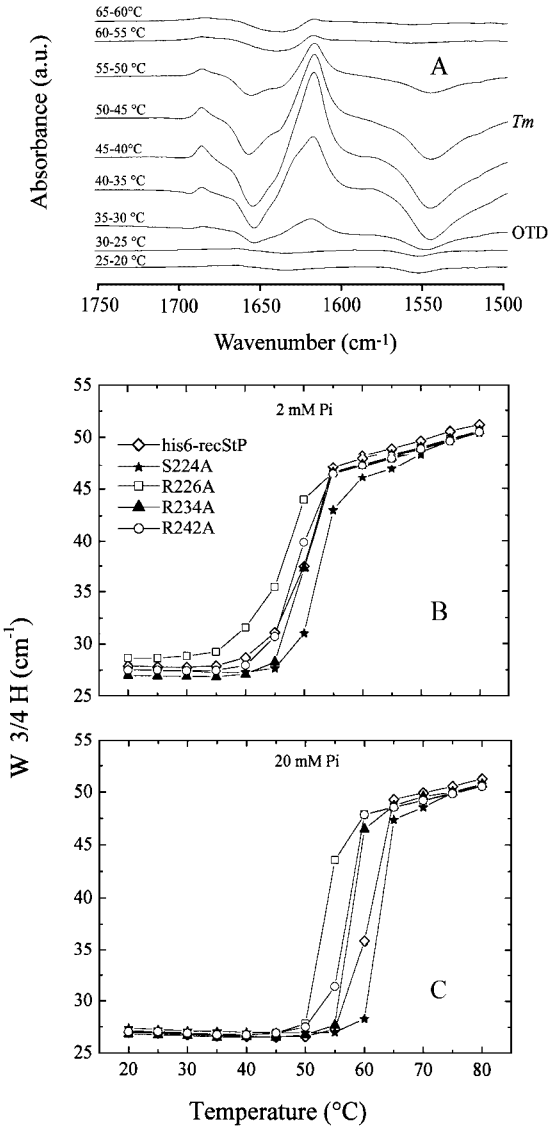

Fig. 5. **Thermal denaturation of his$_6$-recStP and mutants thereof in the presence of different P$_i$ concentrations.** All spectra were obtained in ^2H_2O medium, at p^{2}H 6.8. (A) Thermal denaturation of R226A mutant in 2 mM P$_i$ buffer shown by using difference spectra. Each difference spectrum is the result of the difference between two original absorbance spectra recorded at the temperatures reported (*e.g.*, 25–20°C). The abbreviations are: OTD, onset of thermal denaturation; T_m, melting point. (B, C) Thermal denaturation curves were obtained by monitoring the amide I′ bandwidth, calculated at 3/4 of amide I′ band height (W3/4 H), as a function of the temperature (*3*, *12*).

some caution because a monomeric intermediate escapes detection at higher temperatures when aggregation occurs at a fast rate. However, release of the pyridoxal 5′-phosphate cofactor into solution is a good indication of loss of native oligomeric structure, and this occurs with all mutants in the temperature range of the reported OTD values. Figure 5 (A–C) shows some typical results, and OTD and T_m values are summarized in Table 1. The original thermal denaturation curves (Fig. 5, B and C) were fitted with a sigmoid function from which T_m values were calculated with good precision (*15*).

We begin the discussion by comparing OTD and T_m values seen at a low P$_i$ level because the effect of the mutation is completely unmasked under these conditions. S224A and R234A mutants show higher OTD values than the wild type. Replacement of Arg-226 by alanine has an opposite effect of about the same magnitude on OTD. The R242A mutant appears to be as stable, in terms of OTD, as the wild-type. Therefore, the order of stability derived from the comparison of OTD values is S224A ≈ R234A > his$_6$-recStP ≈ R242A > R226A. Note that structural compactness, measured on the basis of $^1H/^2H$ exchange data, leads to placement of his$_6$-recStP and the mutants in the identical order. Interestingly, the values of T_m show a smaller variation than do the corresponding OTD values. Therefore, this implies that the effect of the mutations is mainly on OTD. As we mentioned above, OTD of StP at least partially reflects loss of functional oligomeric structure (and hence inactivation) under conditions of irreversible thermal denaturation (*3*). Effectively no reversibility of subunit dissociation has been observed when StP was incubated at temperatures of 30°C or higher (*3*). This is probably due to the release of cofactor into dilute solution on the one hand, and partial unfolding and aggregation of the subunits on the other hand. Occurrence of aggregation at elevated temperatures has been corroborated for all proteins studied in this work using light scattering measurements (data not shown). Likewise, release of cofactor into solution could be detected in all cases, using methods described in (*3*). The differences between T_m and OTD values serve to further illustrate the effect of mutation on OTD because they decrease in approximately the same order across the series of proteins in Table 1 as the corresponding OTD values increase.

In the presence of 20 mM phosphate or sulfate, the stabilization brought about by oxyanions is mirrored by marked increases in both OTD and T_m values, compared to the corresponding reference values obtained in 2 mM phosphate buffer. The observed increase in stability is not uniform and depends on both the mutation and the added oxyanion. It is of particular interest to note that the extra stability seen in the S224A and R234A mutants in comparison to his$_6$-recStP when the P$_i$ level was low is almost completely lost in the presence of 20 mM phosphate or sulfate. Two other important pieces of evidence are revealed by a detailed analysis of the data in Table 1. First, except for the S224A mutant in which OTD and T_m values are effected to a comparable extent by added phosphate or sulfate (ΔOTD ≈ 15°C; ΔT_m ≈ 14°C), it is the OTD value that increases most in the presence of oxyanion. Observed ΔOTD values of ≤ 17.5°C compare with ΔT_m values of ≤ 14.5°C. In almost all cases, phosphate has a smaller effect on OTD and T_m than sulfate, which may reflect differences in K_d values of the StP-oxyanion complexes at 30°C (*3*). Second, a difference in the stabilizing effect of the oxyanions in his$_6$-recStP and the mutants is pointed out by comparing the difference between T_m and OTD values. This difference is a maximum under conditions of low P$_i$ and decreases markedly when phosphate and sulfate are present. Comparison of these results with corresponding data for his$_6$-recStP and mutants obtained in the absence of oxyanion reinforce the conclusion that the mutations can complement to a certain extent the

Table 1. **Comparison of stepwise thermal denaturations of his$_6$-recStP and mutants thereof under different buffer conditions.** All buffers had a p^{2}H of 6.8 and contained 2 mM P_i (A), 20 mM P_i (B), or 20 mM Hepes and 20 mM sodium sulfate (C). The abbreviations are: OTD, onset of thermal denaturation; T_m, melting point. Values are derived from analysis of infrared spectra as described in text. At the 95% confidence level, T_m values have calculated standard deviations of ± 0.9°C, ± 0.54°C, and ± 0.45°C in buffers A, B, and C, respectively. OTD values have S.D. of less than ± 0.8°C.

Protein	OTD (°C)			T_m (°C)			T_m – OTD (°C)		
	Buffer			Buffer			Buffer		
	A	B	C	A	B	C	A	B	C
Wild type	40	54	57.5	50	60	61.9	10	6	4.4
S224A	45	59	59.5	52.6	62.2	65.4	7.6	3.2	5.9
R226A	35	49	52.5	46.6	53.2	57.0	11.6	4.2	4.5
R234A	44	54	57.5	49.9	57.5	61.7	5.9	3.5	4.2
R242A	40	50	54	49	56.2	58.3	9	6.2	4.3

Table 2. **Comparison of half-life times ($t_{1/2}$) of his$_6$-recStP and mutants thereof in the absence and presence of stabilizing oxyanion at 45°C.** Data in parentheses are $t_{1/2}$ values obtained at 55°C. n.d., not determined. Half-life times of wild-type StP and the R236A and S238A mutants were identical within the experimental error of <10%. S.D. of linear regression analysis of data plotted in the form, natural logarithm of the remaining enzyme activity against the incubation time. [1]Indicated values are taken from Ref. *5*.

Protein	$t_{1/2}$ (min)		
	No oxyanion added	10 mM phosphate	10 mM sulfate
Wild type	3.2 ± 0.05[1]	stable[1] (2.20 ± 0.15)	stable[1] (5.6 ± 0.6)
S224A	50.0 ± 4.00	stable (26 ± 2.5)	stable
R226A	1.2 ± 0.30	27.0 ± 3.00	n.d.
R234A	20.0 ± 0.40[1]	stable[1] (2.20 ± 0.20)	stable[1] (5.5 ± 1.1)
R242A	11.8 ± 0.30[1]	43.0 ± 5.00[1]	stable[1]

effect of oxyanion binding. The fact that under all conditions T_m values are significantly greater than the corresponding OTD values agrees with the notion of a stepwise denaturation mechanism in which loss of oligomeric integrity (which we suggest is a component of the observable OTD value) precedes the complete unfolding ($\approx T_m$). It also suggests that bound oxyanion leads to a delay of both steps or in other words, it appears to increase the kinetic stabilities of the native association state and the folded structure of the subunit.

Thermal Inactivation Rates of his$_6$-recStP and Mutants Thereof—We have shown recently that the pseudo-first-order rate constant of irreversible thermal inactivation of StP or his$_6$-recStP is a useful reporter of the loss of the native oligomeric structure (*3*, *5*). Therefore, comparisons of half-lives of enzyme activity and OTD values from FT-IR measurements should yield complementary pictures of relative oxyanion-dependent stabilities of his$_6$-recStP and the mutants thereof. Table 2 summarizes half-lives of his$_6$-recStP and mutants and compares data measured in the absence and presence of stabilizing oxyanion. It was confirmed in separate control experiments that measured losses of activity at 45°C are not reversible upon cooling to ambient temperature and incubation for about 1 h. When no oxyanion is added, the order of decreasing kinetic stability is S224A > R234A > R242A > his$_6$-recStP ≈ R236A ≈ S238A > R226A, which generally agrees very well with the corresponding OTD-based or T_m-based order seen under comparable P_i conditions. Under the conditions used, sulfate stabilizes all enzyme activities better than phosphate, and the greatest increase in kinetic stability upon addition of oxyanion is observed for the wild type. Note, however, that preferential stabilization by sulfate is mainly due to tighter apparent binding of sulfate than P_i (*3*, *5*). Again, these observations are in excellent agreement with OTD values in Table 1 and, likewise, T_m data. Establishing a precise correlation of data obtained by these different methods is however difficult, clearly, because of the greater than 1,000-fold difference in protein concentration used in infrared measurements and enzyme assays and its likely impact on a dissociative protein denaturation mechanism such as that of StP.

This work was supported by grants from Austrian Science Funds (P11898-MOB and P15118-MOB to B.N.) and a grant from Università Polytecnica delle Marche (to F.T.). B.P., B.N., and F.T. acknowledge financial support from a grant (no. 21) for technical-scientific collaboration between Austria and Italy. F.-M.P. is a recipient of a PhD grant from the University of Catania, Italy.

REFERENCES

1. Mizoue, L.S. and Chazin, W.J. (2002) Engineering and design of ligand-induced conformational changes in proteins. *Curr. Opin. Struct. Biol.* **12**, 459–463
2. Ahmad, A., Akhtar, M.S., and Bhakuni V. (2001) Monovalent cation-induced conformational change in glucose oxidase leading to stabilization of the enzyme. *Biochemistry* **40**, 1945–1955
3. Griessler, R., D'Auria, S., Tanfani, F., and Nidetzky, B. (2000) Thermal denaturation pathway of starch phosphorylase from *Corynebacterium callunae*: oxyanion binding provides the glue that efficiently stabilizes the dimer structure of the protein. *Protein Sci.* **9**, 1149–1161
4. Griessler, R., Pickl M., D'Auria, S., Tanfani, F., and Nidetzky, B. (2001) Oxyanion-mediated protein stabilization: differential roles of phosphate for preventing inactivation of bacterial α-glucan phosphorylases. *Biocat. Biotrans.* **19**, 379–398

5. Griessler, R., Schwarz, A., Mucha, J., and Nidetzky, B. (2003) Tracking interactions that stabilize the dimer structure of starch phosphorylase from *Corynebacterium callunae*: roles of Arg-234 and Arg-242 revealed by sequence analysis and site-directed mutagenesis. *Eur. J. Biochem.* **270**, 2126–2136
6. Newgard, C.B., Hwang, P.K., and Fletterick, R.J. (1989) The family of glycogen phosphorylases: structure and function. *Crit. Rev. Biochem. Mol. Biol.* **24**, 69–99
7. Weinhäusel, A., Griessler, R., Krebs, A., Zipper, P., Haltrich, D., Kulbe, K.D., and Nidetzky, B. (1997) α-1, 4-D-Glucan phosphorylase of gram-positive *Corynebacterium callunae*: isolation, biochemical properties and molecular shape of the enzyme from solution X-ray scattering. *Biochem. J.* **326**, 773–783
8. Watson, K.A., Schinzel, R., Palm, D., and Johnson, L.N. (1997) The crystal structure of *Escherichia coli* maltodextrin phosphorylase provides an explanation for the activity without control in this basic archetype of a phosphorylase. *EMBO J.* **16**, 1–14
9. Johnson, L.N. (1992) Glycogen phosphorylase: control by phosphorylation and allosteric effectors. *FASEB J.* **6**, 2274–2282
10. Buchbinder, J.L., Rath, V.L., and Fletterick, R.J. (2001) Structural relationships among regulated and unregulated phosphorylases. *Annu. Rev. Biophys. Biomol. Struct.* **30**, 191–209
11. Copley, R.R. and Barton, G.J. (1994) A structural analysis of phosphate and sulfate binding sites in proteins. Estimation of propensities for binding and conservation of phosphate binding sites. *J. Mol. Biol.* **242**, 321–329
12. Skorko-Glonek, J., Lipinska, B., Krzewski, K., Zolese, G., Bertoli, E., and Tanfani, F. (1997) HtrA heat-shock protease interacts with phospholipid membranes and undergoes conformational changes. *J. Biol. Chem.* **272**, 8974–8982
13. Tanfani, F., Galeazzi, T., Curatola, G., Bertoli, E., and Ferretti, G. (1997) Reduced β-strand content in apoprotein B-100 in smaller and denser low-density lipoprotein subclasses as probed by Fourier-transform infrared spectroscopy. *Biochem. J.* **322**, 765–769
14. Mäntele, M. (1993) Reaction-induced infrared difference spectroscopy for the study of protein function and reaction mechanisms. *Trends Biochem. Sci.* **18**, 197–202
15. Meersman, F., Smeller, L., and Heremans, K. (2002) Comparative Fourier transform infrared spectroscopy study of cold-, pressure-, and heat-induced unfolding and aggregation of myoglobin. *Biophys. J.* **82**, 2635–2644